

Microdefects induced by cavitation for gettering in silicon wafer

Dan O. Macodiyo · Hitoshi Soyama ·
Takashi Masakawa · Kazuo Hayashi

Received: 8 February 2006 / Accepted: 31 March 2006 / Published online: 5 August 2006
© Springer Science+Business Media, LLC 2006

The semiconductor industry is not only obsessed by the cleanliness of the processing methods but also the decreasing dimensional scale of components. Contamination, from trace amounts of metals, can alter the electrical properties of silicon devices and even cause them to fail. Gettering, a process in which metallic components are trapped in the bulk of wafer, is used to reduce contamination on the active device surface.

As the critical dimensions for semiconductor devices become smaller, it is becoming necessary to specify precisely the structures, interface morphology, the shape and sizes of individual features, and control at the atomic scale is essential. During semiconductor device processing, microdefects do occur. Microdefects in CZ silicon are known to have both positive and negative effects. If properly controlled, they act as gettering sites for metallic species and hence remove unwanted impurities in the active device regions of semiconductor devices. On the other hand, microdefects can be responsible for plastic deformation of silicon wafer [1]. The occurrence of dislocations in the active device regions causes current leakage and even failure of devices [2]. Determination of the optimum point at which bulk microdefects can be considered to have beneficial gettering effect in silicon wafer is still an engineering concern yet to be resolved.

Many analytical techniques are now been used for studying microdefects in-situ and post fabrication of

semiconductor devices. Transmission electron microscopy (TEM) in combination with advanced specimen preparation machines is an indispensable technique for examining the layered structures, which make up semiconductor devices. In this study, TEM has been used to characterize and image the silicon wafer structure in the atomic scale. The authors have already studied electrical characteristics of backside damage gettering by cavitation impact [3–5]. Despite extensive research in gettering, the exact mechanisms by which mobile dislocations are generated in the bulk of an initially dislocation free silicon wafer are not well understood. The purpose of this study is to analyse types of dislocation misfits and the corresponding defect size that is responsible for effective gettering. Thus, the approach to the structural analysis has been done by considering the cavitation impact process responsible for generating the dislocations mechanism and the associated dislocation misfits analysed using TEM.

Figure 1 shows the test section of the cavitating jet apparatus used for the introduction of backside damage. The surface of silicon wafer was masked with a tape and placed onto specimen holding device and then immersed in DI water. The test liquid, DI water, was injected onto the surface of the specimen through a nozzle, diameter 0.8 mm, with an upstream and downstream pressure of 2.5 and 0.1 MPa, respectively. The standoff distance was 17 mm. The standoff distance s_d , is defined as the distance between the upstream corner of the nozzle throat and the surface of the specimen under test. Hence, the optimum standoff distance s_{opt} is determined qualitatively by an erosion test in which the standoff distance is varied [6]. Details of the cavitating jet in submerged condition are found in references [7–10]. Upon leaving the nozzle, a cavitating jet was formed. The collapsing of the cavitation bubbles causes shock wave and/or microjets on the

D. O. Macodiyo (✉) · K. Hayashi
Institute of Fluid Science, Tohoku University, 2-2-1 Katahira,
Aoba-ku, Sendai 980-8577, Japan
e-mail: dan_macodiyo@yahoo.co.uk

H. Soyama · T. Masakawa
Department of Nanomechanics, Tohoku University, 6-6-01
Aoba, Aramaki, Aoba-ku, Sendai 980-8579, Japan

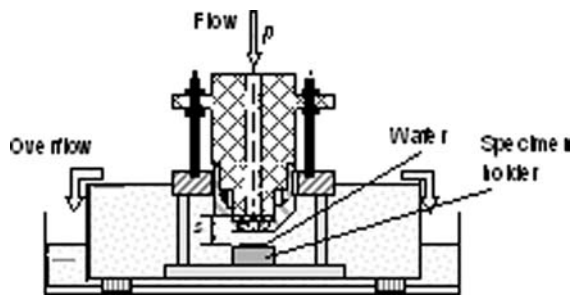


Fig. 1 Test section of cavitation jet apparatus

specimen surface thereby causing suitable plastic deformation. The suitable damage necessitates the gettering site in the bulk of the material, which acts as sink for metallic impurities. The suitable damage was controlled by adjusting hydraulic parameters such as injection pressure of the cavitating jet and standoff distance. The surface of the specimen treated by cavitation impact was observed using atomic force microscope. The threshold deformation and surface roughness was 3.99 and 2.09 nm, respectively.

The specimen was shaped to 5 mm square using a micro-cutter and then cleaned using ethyl alcohol (CH₃CH₂OH). The sample was fixed to a glass using epoxy resin and then mechanically polished to thickness $t = 30 \mu\text{m}$. Final mechanical polishing was done using a dimple grinder to $t = 20 \mu\text{m}$ and then ion-milled at low angle 12°, 3 kV and argon flow 0.3 cm³ until perforation.

Figure 2a shows a mixed type dislocation where complete contrast is not possible. One of the dipole sides has a single line dislocation (S) and a dislocation loop which appears to be the region of the highest cavitation impact. On this particular dipole side, another single dislocation stretches on the lower end. Individual narrow dislocation dipole (D) can also occur as shown in Fig. 2b. The central part of the dipole has a micro Frank–Read dislocation source, which indicates the preferential shearing area. The start of the dislocation dipole is revealed in bright–dark oscillations at the top and bottom with two parallel dislocation lines joining them. The size of the single dislocation and narrow dislocation dipole are 70 and 100 nm, respectively. Double diffraction route was avoided by imaging the silicon on (100) zone as illustrated by the spot diffraction pattern at the bottom insert in Fig. 2a.

Figure 3 shows a strong beam image in bright-field mode of silicon (100). For regions where there was curvature in the dislocation line, the specimen experienced mixed edge- (E) and screw-dislocation (S). On a higher magnification (see circled region), the length of the dislocation loops was 50 nm as marked by position F in Fig. 3. However, there are no dipoles attached to the dislocation loops for this case.

Peculiar curved dislocation segments occurred at the nodes of the dislocation loops as illustrated in Fig. 4. Single cavitation impact may cause multiple disintegration of dislocation loops and thus creating an overlap situation

Fig. 2 Diffraction of single dislocation (S) and a narrow dislocation dipole (D)

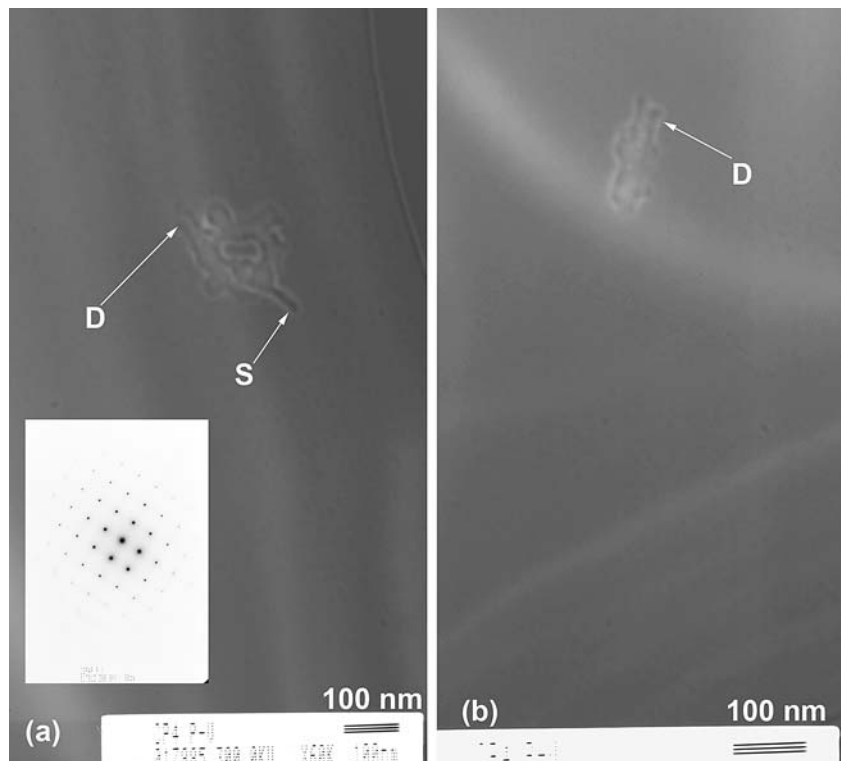
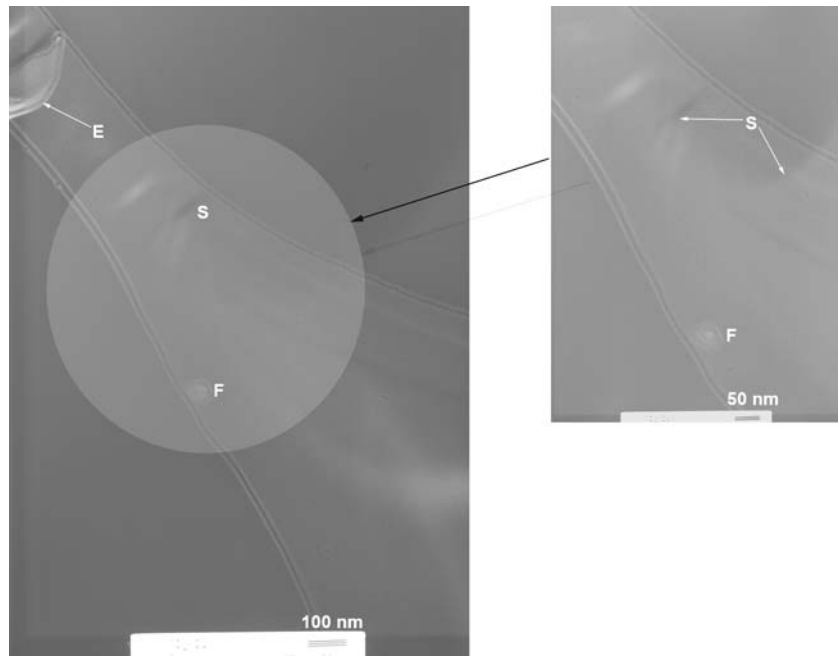


Fig. 3 Strong beam images of edge- (E) and screw (S) orientation



(see region A_1) or single dislocation (see region A_2) in Fig. 4. The dislocation loops are approximately 30 nm. However, the curved strained affiliated to these areas have wider radii. Although the dislocation density was not quantitatively determined, the effect of single cavitation impact can be estimated by the mean tangential distance between the strained cords of A_1 and A_2 .

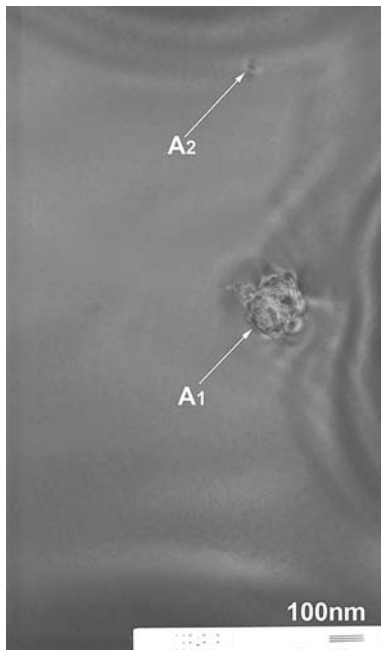


Fig. 4 Curved dislocation segments in silicon (100)

It can be concluded that dislocation dipoles are associated with dislocation loops and are initiated by micro Frank–Read dislocation. Plan-view TEM observations reveal that the size of the dislocation misfits was approximately 100 nm.

Acknowledgement This work was supported by the Japan Society for the Promotion of Science (JSPS) under the Grant No. 16004335. The authors would like to thank Mr. E. Aoyagi and Mr. Y. Hayasaka of the IMR, Tohoku University, for their assistance in TEM observations.

References

1. Leroy B, Plougonven C (1980) *J Electrochem Soc* 127:961
2. Fahey PM, Mader SR, Stiffler SR, Mohler RL, Mis JD, Slinkman JA (1992) *IBM J Res Develop* 36:158
3. Soyama H, Saito S, Macodiyo DO, Koyanagi M (2005) In: *Proceedings of the 2nd international symposium on mechanical science based on nanotechnology*, Sendai, Japan, p 85
4. Kumano H, Sasaki T, Soyama H (2004) *Appl Phys Lett* 85(17):3935
5. Soyama H, Kumano H (2000) *Electrochem Solid-State Lett* 3(2):93
6. Soyama H, Kusaka T, Saka M, Sato A (2000) In: *Proceedings of the 2000 Japanese spring conference for technology plasticity*, Tokyo, p 381
7. Soyama H, Kusaka T, Saka M (2001) *J Mater Sci Lett* 20(13):1263
8. Soyama H, Saito K, Saka M (2002) *Trans ASME, J Eng Mater Technol* 124(2):135
9. Odhiambo D, Soyama H (2003) *Int J Fatigue* 25(9–11):1217
10. Soyama H, Odhiambo D, Saito K (2003) In: *Wagner L (ed) Shot peening*, Wiley-VCH, Weinheim, Germany, p 435